Malaysian Journal of Chemistry, 2024, Vol. 26(5), 273-293
(Special Issue: *3rd Virtual International Symposium on Sciences 2023*)

Molecular Docking Studies of Phytochemicals from *Curcuma longa* against Trehalose-6-Phosphate Phosphatases of Pathogenic Microbes

Nurul Anis Johari[1], Adam Azmihan[1], Mohamad Zakkirun Abdullah[2] and Latifah Munirah Bakar[1]*

[1]School of Biology, Faculty of Applied Sciences, Universiti Teknologi MARA, Shah Alam, 40450 Shah Alam, Selangor, Malaysia

[2]Department of Fundamental Dental and Medical Sciences, Kulliyyah of Dentistry, International Islamic University Malaysia, 25200 Kuantan, Pahang, Malaysia

*Corresponding author (e-mail: latifahmunirah@uitm.edu.my)

Trehalose-6-phosphate phosphatases (TPP) are crucial enzymes used by pathogenic microbes for trehalose sugar biosynthesis, which is later beneficial for infection and proliferation. Therefore, inhibition of TPP proteins becomes the main focus for combating pathogenic microbial infection. This study aims to investigate the binding interactions between selected phytochemicals from *Curcuma longa* against TPP enzymes regarding the binding affinities and the presence of non-covalent interactions using molecular docking software. Molecular docking of *C. longa* phytochemicals against TPP was performed utilizing various software, including PyMol, Discovery Studio Biovia 2021, AutoDock Vina, and AutoDock Tools version 1.5.7. *In silico* molecular docking analysis using AutoDock Vina was done to predict the binding energy and interactions of 30 ligands that belong to *C. longa* with TPP proteins from *Cryptococcus neoformans* (PDB: 5DX9), *Candida albicans* TPP C-terminal domain (PDB: 5DXI) and TPP from *Salmonella typhimurium* in complex with trehalose (PDB: 6UPD), whereas ampicillin, fluconazole and isoniazid act as the drugs control. The three-dimensional (3D) models of TPP docked with 30 phytochemicals revealed that most of them have good binding affinities to the TPP enzyme. Interestingly, anthraquinones exhibited among the highest binding affinities, ΔG: -8.4, -8.1 and -7.5 kcal/mol. In addition, quercetin is one of the ligands that exhibit the strongest binding affinity, which is -9.3 kcal/mol interaction between TPP from *C. neoformans*, and affinity binding of -7.3 and -6.2 kcal/mol interaction with TPP from *C. albicans* and *S. typhimurium* respectively. These findings suggest that turmeric phytochemicals have some potential to act as TPP inhibitors, which could contribute toward the future development of new drugs against TPP-producing pathogenic microbes. The data presented warrant validation using in vitro and in vivo assays.

Keywords: Trehalose-6-phosphate phosphatases; *Curcuma longa*; phytochemicals, molecular docking; binding affinity; new generation drugs

Received: November 2023; Accepted: February 2024

A stress-protective molecule, trehalose is an essential sugar in most organisms, including bacteria, invertebrate animals, fungi, and plants [1]. The trehalose biosynthesis pathway involves a series of reactions between trehalose-6-phosphate synthase (TPS) and trehalose-6-phosphate phosphatase (TPP). Trehalose-6-phosphate phosphatase catalyzes the dephosphorylation of trehalose-6-phosphate (T6P) to trehalose and orthophosphate. Trehalose, a disaccharide commonly found in bacteria, fungi, and invertebrates, is critical for organism survival under stressful conditions [2]. Humans and animals are exposed to the pathogenicity of the above pathways. Many serious diseases such as tuberculosis, aspergillosis, and pandemic diseases are leading causes of death worldwide, most of which are mediated by the affected pathogen TPP. Thus, trehalose phosphate phosphatase has been implicated as a major virulence molecule in most pathogenic microbes [3].

Antibiotic or drug resistance caused by pathogens is a prominent issue in modern medicine associated with drug abuse [4]. Aside from the pathogen's virulence, antimicrobial resistance (AMR) has arisen among the most significant outcome causes in patients with severe infections [5]. The key to solving the problems is to target signaling pathways or genes shared by pathogens but absent in the host. There are specific prescription medications, but genes like the trehalose pathway and TPP affect specific pathogens, not humans or animals. The discovery of TPP-specific inhibitors' therapeutic potential in treating other bacterial, fungal, and parasitic diseases is gradually becoming a highly active area of biomedical research [1].

†Paper presented at the 3rd Virtual International Symposium on Sciences (3rd VISoS 2023)

Plant-based phytochemicals provide appealing, beneficial, and comprehensive drug effects against pathogens without significant side effects. *C. longa* has beneficial compounds that have been linked to improved health. Chemical constituents of turmeric, such as cyclocurcumin and curcumin, have been described as potent antioxidant, anti-inflammatory, antibacterial, antifungal, and antiviral agents [6]. In other words, these compounds can exert antibacterial properties against several pathogenic microorganisms. Therefore, it is important to examine the effectiveness of probable phytochemicals as therapeutic molecules against TPP and to screen them [7].

The approach of drug design based on the structure using phytochemicals helps lower related imprecision and speed up the process [8]. Molecular docking is an in-silico approach that has become a crucial tool for developing a wide variety of new drugs, helping researchers understand the optimal interactions between proteins and ligands [1]. This approach predicts how enzymes of proteins interact with small molecules (ligands) and analyzes the ligand-protein binding pose, conformation, orientation, binding free energy, and binding affinity [2].

Concern about virtual ligand-protein interaction models at the atomic level can be later confirmed using in vitro and in vivo approaches, saving time, energy, and costs. As a result, the research focuses on the *in silico* docking of phytochemicals chosen as lead molecules to validate their binding affinities to the modelled TPP protein regarding known antimicrobial agents. This could aid in developing next-generation drug cues against the virulent TPP, which is involved in the infection and spread of numerous pathogens [9].

Previous studies have shown the antimicrobial activity of each constituent of *Curcuma longa*, showing the potential as an antimicrobial agent. It has a drawback because numerous compounds must be examined in the laboratory. By inhibiting trehalose-6-phosphate phosphatase, it may be possible to regulate metabolic pathways and potentially treat diseases or conditions associated with dysregulated metabolism. Molecular docking is crucial in developing novel drugs to predict protein interaction with potential drugs before proceeding with traditional in vitro and in vivo assays. However, a lack of study has been performed to predict the interaction between *C. longa* bioactive compounds and TPP target protein in molecular docking. Hence, molecular docking between the active constituents of C. longa and the TPP protein needs to be performed to preserve time, energy, and cost. Besides, molecular docking is an important tool in developing novel drugs to predict the protein interaction with potential drugs before proceeding with traditional assays in vitro and in vivo.

Docking enables the virtual screening of databases of approved pharmaceuticals, natural products, or previously synthesized compounds for one or more biological targets of interest in a reasonable amount of time. A substantial effort will be made in this work to develop new generation candidate medications that inhibit TPP using *in silico* techniques. The *in-silico* designing strategy employed in this study aided in recognizing some lead molecules, which may further explain their resolution for further purposes, such as *in vitro* and *in vivo* evaluations [10].

Next, increasing efforts have been made to improve docking algorithms and overcome their inherent limitations. The binding energy (binding affinity/Gibbs energy, ΔG) is obtained during the docking process, a parameter of the conformational stability between the ligand and the receptor. Interacting ligands and receptors are usually in the lowest energy state, where protein-ligand binding occurs spontaneously. This state causes the molecule to be in a stable state. Thus, negative ΔG scores indicate the stability of emerging complexes with receptor molecules, an important property of effective drugs [11].

EXPERIMENTAL

Research Materials: Software and Program

PyMol and Discovery Studio Biovia 2021 were used to visualize and modify the structures of receptors and ligands. AutoDock Vina was the main docker used in this work. The .PDBQT file format preparation and grid box determination were done with AutoDock Tools version 1.5.7. Post-docking analysis was performed using PyMol and DS Biovia 2021 [10].

Methodology

1. Preparation of Ligand Structures of Phytochemicals from *Curcuma Longa*

The 3D structures of phytochemicals from *Curcuma longa* (*in silico* control) were published online in the Spatial Data File as .SDF file format. The public database PubChem (https://pubchem.ncbi.nlm.nih.gov) was used to access information on the chemical compounds database. The .SDF file format was transformed to the Protein Data Bank Files (.PDB) format using Discovery Studio Biovia 2021. The ligand structure was then prepared with Gasteiger modifications and rotatable bonds using AutoDock Tools 1.5.7. The structures were first transformed from the .PDB file format to the Protein Data Bank, Partial Charge & Atom Type (.PDBQT) file format using ADT, and then AutoDock Vina was used to make the structures suitable for molecular docking [10, 11].

2. Preparation of the Macromolecular Structure of the TPP Protein

The crystal structure of the TPPs protein (PDB: 5DXI, 5DX9, 6UPD) was downloaded from the Research

Collaboratory for Structural Bioinformatics website (http://www.rcsb.org). Protein inhibitors were separated using *Discovery Studio Biovia 2021* and used in the redocking step. ADT software was used to prepare the required files for *AutoDock Vina* by removing water, adding polar hydrogen, computing Gasteiger charges to protein structures, and converting protein structures from the .PDB file format to .PDBQT file format.

3. Grid Box Determination

The grid box's placement was determined based on the known location of the original inhibitor using ADT [11]. The grid coordinates were confirmed after serial redocking steps of the inhibitor to the protein. The root-mean-square deviation (RMSD) value below 2 Ångström (Å) represented the good reproduction of the correct pose of predicted structural conformation as compared to observed structural conformation from actual experiments. In the meantime, the dimensions of each ligand were used to calculate the grid size [10].

4. The Molecular Docking Method

The AutoDock Vina program was used to carry out molecular docking. The output had to be prepared using ADT. The .PDBQT file for the ligand was used to set the size and center of the grid box. The grid center was assigned at x, y, and z dimensions of -15.690, 14.488, and -9.525, respectively, with a grid spacing of 1.000. The grid size dimension was established at 14 x 24 x 12 (x, y, and z) points. The .PDBQT file format was used to store the prepared document. Based on the AutoDock Vina scoring system, negative Gibbs free energy (ΔG) scores (kcal/mol) were predicted for ligand-binding affinities [10,11].

The expected binding affinity indicated the strength of the ligand's binding to the receptor. The post-docking analyses were visualized using PyMOL and Discovery Studio Biovia 2021, showing the sizes and positions of binding sites, hydrogen-bond interactions, hydrophobic interactions, and bonding distances. Each ligand's binding positions were examined, and their interactions with the protein were described. Each ligand's optimal and most energetically advantageous conformations were then chosen [10].

RESULTS AND DISCUSSION

Ligands from *Curcuma longa*, Drugs Control, and Trehalose-6-Phosphate Phosphatase Interaction

Trehalose-6-phosphate phosphatases (TPP) play a significant role in the initiation and virulence of many previously mentioned bacterial, fungal, and nematode infections. Using docking, an extensive simulation was conducted to identify and select phytochemicals against TPPs based on their therapeutic properties. About 30 phytochemicals from *Curcuma longa* were selected for their antifungal and antibacterial potential [10]. Phytochemicals of such high medicinal value can also be expected to have anti-TPP activity since the TPP family of enzymes is involved in the infection and pathogenicity of several bacteria, fungi, and nematodes. The trehalose pathway, in general, and TPPs provide an excellent platform for drug development, as the trehalose pathway is completely absent in animals [1]. Thus, TPP is a promising potential target molecule not only for controlling pathogenic microbes but also for eliminating the presence of multiple resistant strains.

Roles of Trehalose Inhibition in Protection Against Stress

Based on the previous study [1], trehalose-6-phosphatase is an enzyme involved in trehalose metabolism, and its inhibition or modulation can affect the treatment of certain diseases. Since many pathogenic microbes rely on trehalose as a source of energy and protection against environmental stress, the absence of the trehalose pathway in multicellular organisms may be useful in preventing the spread of disease. These organisms may be less susceptible to certain diseases if they cannot produce trehalose [1].

The development of new antibacterial agents may also involve targeting microbial trehalose. The absence of the trehalose pathway in pathogenic microbes can be useful in controlling the pathogen in several ways. The loss of trehalose metabolism is associated with decreased bacterial pathogenicity [12]. This suggests that affecting the trehalose synthesis pathway could potentially reduce the virulence of pathogenic microbes.

Besides, trehalose metabolism is essential for the growth and virulence of globally important pathogens such as *Mycobacterium tuberculosis* [13, 14]. Since humans and other mammals lack trehalose metabolism, it is an attractive target for drug development [13,14]. Targeting the trehalose pathway in pathogens may make it possible to develop drugs that specifically inhibit their growth and virulence. In addition, trehalose has been found to contribute to osmotic stress tolerance in certain pathogens [15]. Compatible solutes like trehalose can help pathogens survive in osmotically challenging environments such as brackish water [15]. By disrupting the trehalose synthesis pathway, it may be possible to weaken the ability of pathogens to withstand osmotic stress, making them more susceptible to control measures.

A study showed that inhibition of trehalose biosynthesis in *Staphylococcus aureus* increased the sensitivity of the bacteria to antibiotics [12]. This suggests that targeting the trehalose pathway could potentially improve the effectiveness of existing antibiotics against pathogenic microbes. Thus, the absence of the trehalose pathway in pathogenic microbes offers opportunities to weaken their virulence, develop targeted drugs, weaken osmotic stress tolerance, and improve the effectiveness of existing

antibiotics. Understanding and manipulating trehalose metabolism in pathogens may allow them to control their growth and virulence more effectively.

In silico Molecular Docking Analyses

The molecular docking was performed to determine the interaction of 30 ligands with the three structures of trehalose-6-phosphatase, which are from *Cryptococcus neoformans* (PDB: 5DX9) and the C-terminal domain from *Candida albicans* (PDB: 5DXI) and *Salmonella typhimurium* in complex with trehalose (PDB: 6UPD).

Molecular docking programs have become an increasingly popular approach to new drug development, partly because of the favorable time and financial costs of *in silico* drug screening compared to traditional laboratory testing. It is a computational method that effectively tries to predict the binding interaction between macromolecules (receptors) and ligands [11].

Docking has proven to be a valuable tool in understanding the interactions between chemical compounds and their molecular targets and in drug discovery and development since its inception in the mid-1970s. Indeed, the number of studies using molecular docking to identify the structural determinants required for efficient ligand-receptor binding and to develop more accurate docking methods has significantly increased since its initial appearance [16].

Next, increasing efforts have been made to improve docking algorithms and overcome their inherent limitations. During the docking process, the binding energy (binding affinity/Gibbs energy, ΔG) is obtained, a parameter of the conformational stability between the ligand and the receptor. Interacting ligands and receptors are usually in the lowest energy state, where protein-ligand binding occurs spontaneously. This state causes the molecule to be in a stable state. Thus, negative ΔG scores indicate the stability of emerging complexes with receptor molecules, an important property of effective drugs [11].

In addition, non-covalent molecular interactions such as hydrogen bonding and hydrophobic and electrostatic interactions to essential amino acid residues also indicate ligand binding in favorable conformations [11]. All these interactions equally affected conformation and binding affinity.

Ampicillin, Fluconazole, and Isoniazid as the Control Agents

Control agents for this molecular docking are ampicillin, fluconazole, and isoniazid. Ampicillin is a beta-lactam antibiotic classified as an aminopenicillin used to control and treat certain bacterial infections [17]. It belongs to the penicillin class of drugs and was developed to address the drug resistance problem and extend its antimicrobial coverage. Next, fluconazole is an antifungal medication used to treat and prevent fungal infections. It works by stopping the growth of fungi [18]. Isoniazid is an antibiotic used to treat mycobacterial infections, most commonly tuberculosis. It is bactericidal when mycobacteria grow rapidly and bacteriostatic when mycobacteria grow slowly. Isoniazid is used to treat meningitis and infections of the larynx, sinuses, lungs, genitals, urinary tract, and gastrointestinal tract [18].

Root Mean Square Deviation (RMSD)

According to a study in 2022 [19], the root means square deviation (RMSD), typically the beginning frame or the crystallographic structure, is the average atom displacement with respect to a reference structure at a certain moment in the simulation. RMSD is computed as a critical parameter to examine the equilibration of MD trajectories [19]. More hydrophobic energy is present when the RMSD is higher, and less hydrophobic energy is present when the RMSD is lower. Strong hydrogen bonding contacts and strong hydrophobic non-bonding interactions in proteins have been found to be the cause of the lower RMSD value [20]. This study calculates the RMSD values for interactions between the ligands and TPP proteins due to molecular docking analyses.

Docking Validation

The grid box size and center coordinates should be validated in molecular docking to ensure the ligand binds to the binding pocket in the correct conformation. A drug control molecule can bind to the receptor of interest and is used as a reference molecule to validate the docking method. It is usually chosen based on its known binding affinity and crystallographic structure. The ligand should have a well-defined binding mode and represent ligands expected to bind to the target protein [21]. Docking validation was performed in this study by re-docking the crystal structure of each inhibitor or original ligand bound to the protein binding site [10].

Molecular Docking Results Between *Curcuma longa* Phytochemicals and TPP Receptor from *Cryptococcus neoformans* (PDB: 5DX9)

First, docking validation was performed by redocking all *Curcuma longa* ligands with *Cryptococcus neoformans* trehalose-6-phosphate phosphatase receptor (PDB: 5DX9). Docking was done on a grid of x = 10, y = 8, z = 12 centered at x = −0.068, y = 22.403, z = 19.44 at 1,000 Angstroms (Å).

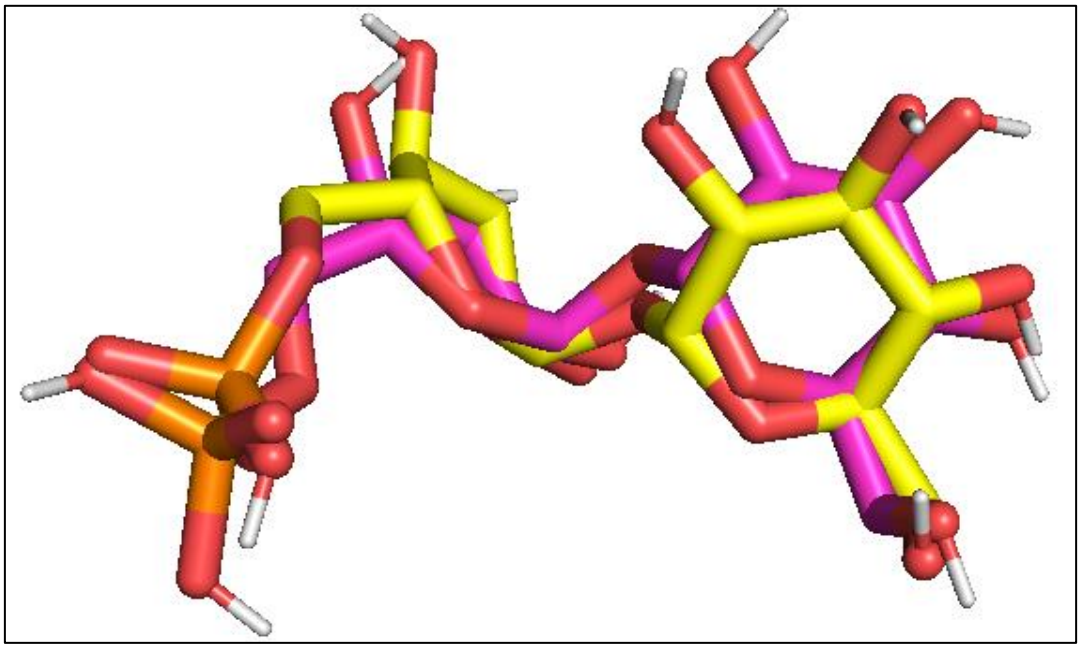

Figure 1. Redocked (yellow) and the crystal structure of trehalose (pink).

Figure 1 below shows the redocking results for trehalose-6-phosphate (T6P) (yellow) and the crystal confirmation of trehalose-6-phosphate phosphatase (pink). The overlay fits between the redocking ligand (yellow) and the T6P crystal form (pink), depicting the location of the binding site between the ligand and the receptor. The root-mean-square deviation (RMSD) value for this interaction is 1.29 Å. Using a computational method, the RMSD was often used to measure the quality of reproduction of a known crystallographic bond position.

A low RMSD means a good reproduction of the correct binding position, according to a previous study [19]. The optimal RMSD in this situation is less than 1.5 Angstrom, or even better, less than 1 Angstrom, regarding the genuine binding position. The lower energy scores represent better protein-ligand binding affinity than the higher energy values. The projected values are more closely aligned with the actual values when the RMSD is lower. As a result, a smaller RMSD score often means the model is more accurate [19].

Binding Affinity Value Between Ligands with TPP from *C. neoformans*

Molecular docking was run for all 30 ligands and the TPP output, both in .PDBQT format. Based on Table 1, the 30 ligands docking with TPP from *Cryptococcus neoformans* show that quercetin resulted in the highest binding affinity of -9.3 kcal/mol, which is higher than recommended drugs, ampicillin, fluconazole, and isoniazid. The docking between TPP and three control drug ligands, ampicillin produced the highest binding affinity, which is -8.8 kcal/mol, and redocking performed by T6P resulted in affinity binding of -10.4 kcal/mol. These results indicate that T6P possesses the highest binding affinity for TPP from *C. neoformans*.

Binding Conformation Based on Hydrogen, Hydrophobic and Electrostatic Interaction Between Ligands and TPP from *C. neoformans*

During the analyses, hydrogen-bonded TPP amino acid residues and hydrophobic and electrostatic interactions with ligands were recorded using Auto Dock Vina. Figure 2 shows the binding conformation of the compounds using PyMol and Discovery Studio Biovia 2021, while Figures 3, 4, and 5 show the 2D illustration of the TPP complex interaction using Discovery Studio Biovia 2021.

Table 1. The binding affinity of ligand molecules to modeled TPP, 5DX9 using *AutoDock Vina*.

Ligand	**Binding energy (binding affinity) generated between ligand and TPP receptor in each form, ΔG (kcal/mol)**								
	1	**2**	**3**	**4**	**5**	**6**	**7**	**8**	**9**
Trehalose-6-Phosphate	-10.4	-9.7	-9.4	-9.4	-9.1	-9.1	-8.8	-8.6	-8.3
Ampicillin	-8.8	-7.8	-7.8	-7.5	-7.0	-6.8	-6.6	-6.4	-
Fluconazole	-8.3	-8.3	-8.1	-8.1	-8.1	-7.9	-7.7	-7.7	-7.6
Isoniazid	-6.3	-6.2	-6.1	-5.7	-5.6	-5.6	-5.6	-5.5	-5.4
Anthraquinones	-8.4	-8.4	-8.4	-8.3	-7.9	-7.9	-7.9	-7.9	-7.8
Ar-tumerone	-7.1	-7.0	-6.9	-6.9	-6.8	-6.8	-6.8	-6.6	-6.5
Bisacurone	-7.8	-7.6	-7.6	-7.5	-7.4	-7.4	-7.3	-7.3	-7.3
Bisdemethoxy-curcumin	-8.7	-8.4	-8.1	-8.0	-7.5	-6.6	-6.4	-6.4	-5.9
Borneol	-5.8	-5.7	-5.7	-5.7	-5.6	-5.6	-5.5	-5.4	-5.4
Caffeic acid	-7.1	-7.1	-7.0	-6.9	-6.6	-6.5	-6.5	-6.4	-6.2
Cis-curcumin	-8.5	-8.4	-8.3	-8.1	-7.3	-7.2	-6.6	-6.6	-6.5
Coumaric	-8.5	-8.4	-7.9	-6.8	-6.8	-	-	-	-
Coumarin	-6.8	-6.6	-6.3	-6.2	-6.0	-6.0	-5.9	-5.9	-5.8
Curcumin	-8.6	-8.6	-8.5	-7.5	-7.4	-7.4	-7.3	-7.1	-6.9
Curcumin Beta-D-glucuronide	-6.0	-4.5	-4.2	-4.0	-3.5	-	-	-	-
Curcuphenol	-6.7	-6.7	-6.4	-6.3	-6.3	-6.2	-6.1	-6.0	-5.9
Curdione	-7.9	-7.8	-7.7	-7.6	-7.6	-7.6	-7.3	-6.9	-6.1
Curlone	-7.2	-7.0	-7.0	-6.9	-6.8	-6.8	-6.8	-6.7	-6.7
Cyclocurcumin	-2.9	-1.1	-0.5	-0.5	-	-	-	-	-
Demethoxy-curcumin	-8.8	-8.5	-8.3	-7.9	-7.5	-6.6	-	-	-
Furanodienone	-7.8	-7.6	-7.5	-7.4	-7.0	-6.9	-6.8	-6.8	-6.8
Germacrone	-8.2	-7.8	7.4	-7.0	-6.6	-6.3	-6.3	-6.0	-5.9
Hexahydro-curcumin	-8.5	-8.5	-8.4	-8.4	-8.3	-8.2	-8.0	-8.0	-8.0
Hexahydrocurcuminol	-8.9	-8.7	-8.7	-8.6	-8.6	-8.6	-8.4	-8.4	-7.8
Isocurcumenol	-8.1	-8.0	-7.9	-7.8	-7.7	-7.4	-	-	-
Isorhamnetin	-9.1	-9.0	-9.0	-8.7	-7.9	-7.9	-7.8	-7.7	-7.3
P-hydroxybenzoic acid	-6.1	-6.0	-5.9	-5.8	-5.8	-5.7	-5.7	-5.6	-5.6
Quercetin	-9.3	-9.0	-8.8	8.5	-8.0	-7.6	-6.5	-6.4	-
Sinapic acid	-7.1	-7.0	-6.7	-6.7	-6.7	-.65	-6.5	-6.5	-6.3
T-cinnamic acid	-6.2	-6.2	-6.0	-6.0	-6.0	-5.9	-5.6	-5.6	-5.4
Turmerone	-7.1	-7.1	-7.0	-6.8	-6.7	-6.6	-6.5	-6.5	-6.4
Vanillic acid	-6.7	-6.6	-6.5	-6.3	-6.2	-6.0	-5.8	-5.8	-5.8
Zederone	-8.7	-8.2	-7.9	-7.6	-7.5	-7.3	-7.3	-7.1	-6.7
Zingiberene	-6.1	-6.1	-5.9	-5.9	-5.8	-5.8	-5.8	-5.7	-5.7

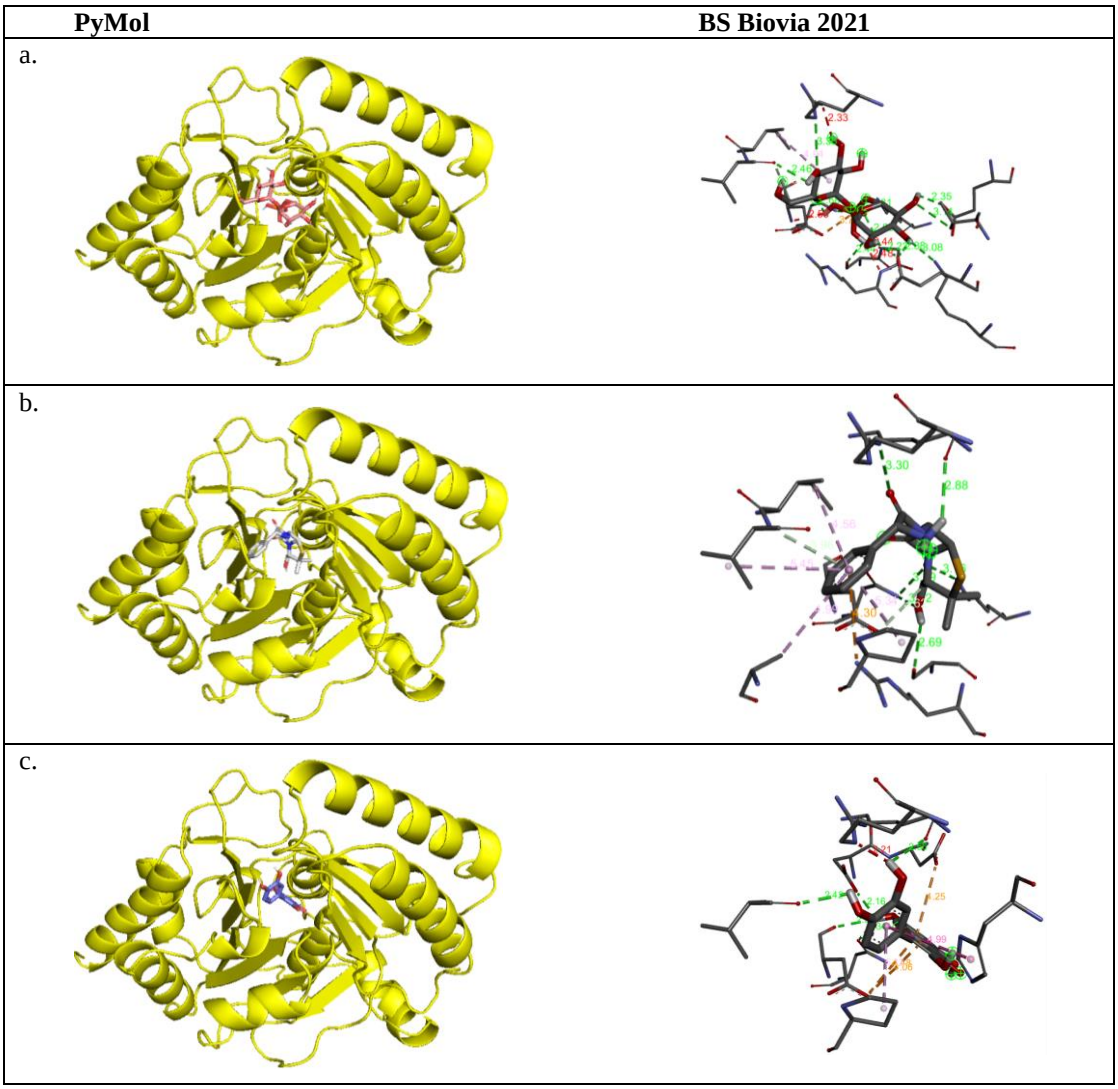

Figure 2. The binding visualization of 5DX9 receptors and ligands.
a. Trehalose-6-phosphate b. Ampicillin c. Quercetin.

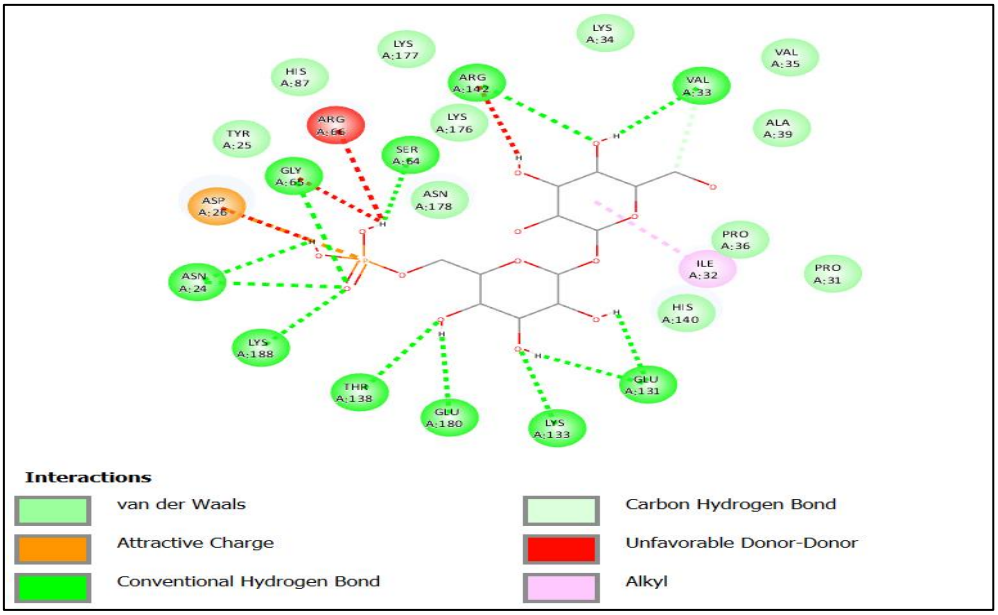

Figure 3. The 2D illustration of docked T6P-5DX9 complex interaction visualization by DS Biovia 2021.

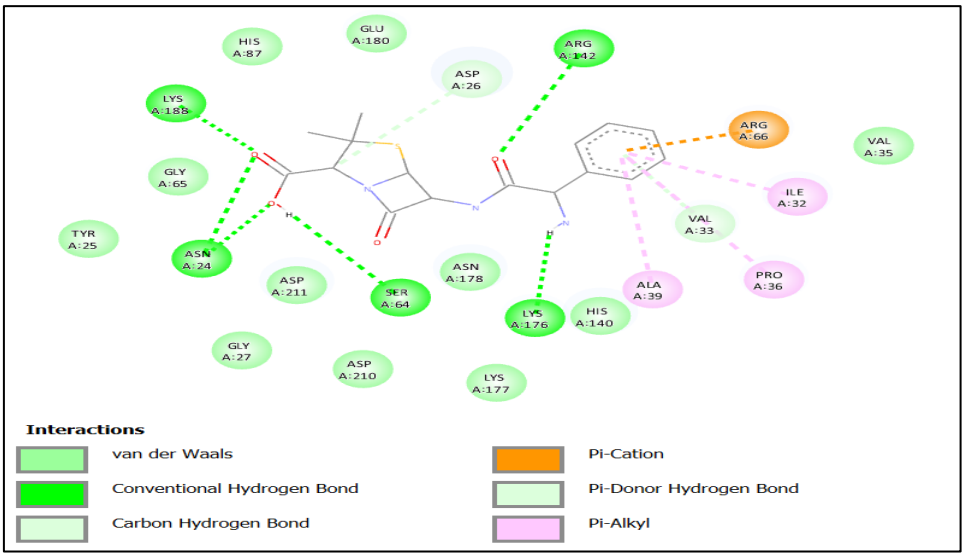

Figure 4. The 2D illustration of docked ampicillin-5DX9 complex interaction visualization by Discovery Studio Biovia 2021.

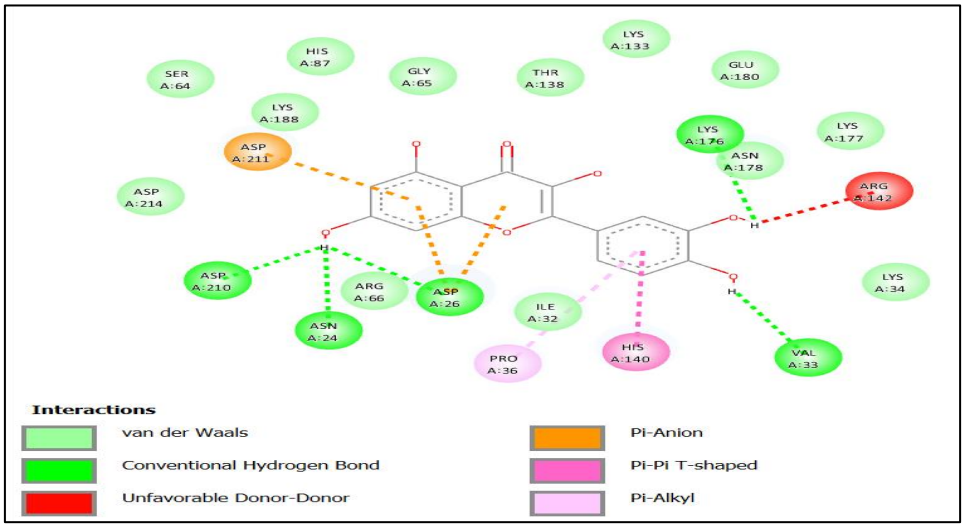

Figure 5. The 2D illustration of docked quercetin-5DX9 complex interaction visualization by Discovery Studio Biovia 2021.

As a result, the Table 2 shows the interaction between T6P with 5DX9 receptor were supported by 13 hydrogen bonds at residues GLU131 (2.23 Å), GLU131 (2.38 Å), GLU180 (2.35 Å), ASN24 (2.68 Å), SER64 (2.44 Å), VAL33 (2.46 Å), ASN24 (3.13 Å), GLY65 (2.85 Å), LYS133 (3.08 Å), THR138 (3.14 Å), ARG142 (3.35 Å), LYS188 (2.81 Å) and VAL33 (3.51 Å) That play a crucial role in ligands binding; and by one hydrophobic interaction at residues ILE32 (4.94 Å). An electrostatic interaction was also identified with ASP26 (3.70 Å).

Eight hydrogen bonds between ampicillin compounds and 5DX9 receptor were established, involving the amino acids LYS176 (2.88 Å), SER64 (2.69 Å), ASN24 (3.39 Å), ASN24 (3.12 Å), ARG142 (3.30 Å), LYS188 (3.16 Å), ASP26 (3.62 Å) and VAL33 (3.96 Å). While this was going on, four hydrophobic interactions involving the amino acids ILE32 (4.56 Å), VAL33 (5.45 Å), PRO36 (5.34 Å) and ALA39 (5.00 Å) took place. When ampicillin and 5DX9 interacted, an electrostatic interaction involving the amino acid Arg66 at 4.30 Å occurred.

As evidenced in Table 2, the interaction between quercetin and 5DX9 receptor, the five amino acids which are LYS176 (2.56 Å), VAL33 (2.42 Å), ASN24 (2.34 Å), ASP26 (2.55 Å) and ASP210 (2.16 Å) formed a hydrogen bond. The amino acids HIS140 and PRO36 also interact hydrophobically, with distances of 4.99 Å and 5.12 Å, respectively. There was additional evidence of electrostatic interaction with ASP26 (4.06 Å), ASP26 (4.48 Å), and ASP211 (4.25 Å).

Molecular Docking Results Between *Curcuma longa* Phytochemicals and TPP C-Terminal Domain from *Candida albicans* (PDB: 5DXI)

The next docking validation was performed by redocking all *Curcuma longa* ligands with the receptor of trehalose-6-phosphate phosphatase C-Terminal from *Candida albicans* (PDB: 5DX9). Redocking was executed with a grid box of size x=6, y=8, z=10, and center x=14.747, y=100.715, z=190.947 at 1,000 Angstroms (Å).

Figure 6 below shows the results of redocking inhibitor trehalose (yellow) and crystal conformation of trehalose (pink). The superimposition fits between the redocking ligand (yellow) and the crystal conformation (pink), which describes the position of the binding site between the ligand and the receptor. The RMSD value is 0.907 Å. RMSD has often been used to measure the quality of reproduction of a known crystallographic binding pose by a computational method. Thus, the lower the RMSD, the better the reproduction of the correct binding pose.

Table 2. Amino acid residues implicated in hydrogen bonding, hydrophobic contacts, and electrostatic interactions, respectively, between the ligands and the TPP from *C. neoformans*.

Ligand	Binding Affinity, ΔG (kcal/mol)	Amino Acids Involved and Distance (Å)		
		Hydrogen Bonding Interaction	Hydrophobic Interaction	Electrostatic Interaction
T6P	-10.4	GLU131 (2.23), GLU131 (2.38), GLU180 (2.35), ASN24 (2.68), SER64 (2.44), VAL33 (2.46), A SN24 (3.13), GLY65 (2.85), LYS133 (3.08), THR138 (3.14), ARG142 (3.35), LYS188 (2.81), VAL33 (3.51)	ILE32 (4.94)	ASP26 (3.70)
Ampicillin	-8.8	LYS176 (2.88), SER64 (2.69), ASN24 (3.39), ASN24 (3.12), ARG142 (3.30), LYS188 (3.16), ASP26 (3.62), VAL33 (3.96)	ILE32 (4.56), VAL33 (5.45), PRO36 (5.34), ALA39 (5.00)	ARG66 (4.30)
Quercetin	-9.3	LYS176 (2.56), VAL33 (2.42), ASN24 (2.34), ASP26 (2.55), ASP210 (2.16)	HIS140 (4.99), PRO36 (5.12)	ASP26 (4.06), ASP26 (4.48), ASP211 (4.25)

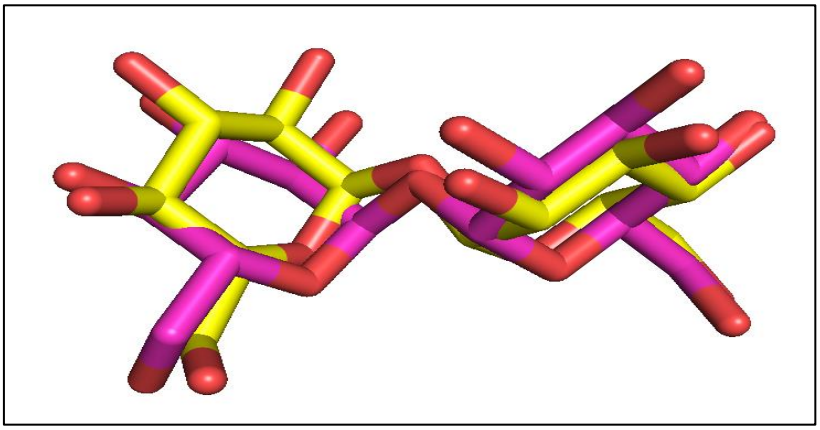

Figure 6. Redocked (yellow) and the crystal structure of trehalose (pink).

Table 3. The binding affinity of ligand molecules to modeled TPP, 5DXI using *AutoDock Vina*.

Ligand	Binding energy (binding affinity) generated between ligand and TPP receptor in each form, ΔG (kcal/mol)								
	1	**2**	**3**	**4**	**5**	**6**	**7**	**8**	**9**
Trehalose	-8.3	-8.3	-8.3	-8.2	-7.4	-7.3	-7.2	-6.5	-6.0
Ampicillin	-6.7	-5.5	-5.2	-5.0	-3.9	-	-	-	-
Fluconazole	-7.9	-7.8	-7.7	-7.7	-7.1	-6.8	-6.7	-6.1	-5.9
Isoniazid	-5.6	-5.5	-5.4	-5.4	-5.3	-5.3	-5.3	-5.3	-5.2
Anthraquinones	-8.1	-8.1	-8.1	-8.1	-7.6	-7.6	-7.5	-7.4	-6.8
Ar-tumerone	-6.5	-6.5	-6.4	-6.4	-6.4	-6.1	-5.8	-5.8	-5.7
Bisacurone	-7.6	-7.5	-7.3	-7.3	-7.1	-7.0	-7.0	-6.4	-6.3
Bisdemethoxycurcumin	-7.0	-6.1	-6.0	-5.1	-4.4	-	-	-	-
Borneol	-5.3	-5.3	-5.3	-5.2	-5.0	-5.0	-5.0	-5.0	-4.9
Caffeic acid	-7.1	-6.5	-6.5	-6.2	-6.1	-6.0	-6.0	-6.0	-6.0
Cis-curcumin	-7.4	-6.7	-6.4	-4.9	-4.5	-	-	-	-
Coumaric	-5.1	-	-	-	-	-	-	-	-
Coumarin	-6.3	-6.2	-6.0	-6.0	-5.9	-5.9	-5.8	-5.8	-5.7
Curcumin	-5.6	-4.0	-2.9	-2.8	-	-	-	-	-
Curcumin Beta-D-glucuronide	6.5	-	-	-	-	-	-	-	-
Curcuphenol	-6.4	-6.1	-6.1	-6.1	-6.1	-6.0	-6.0	-6.0	-5.7
Curdione	-7.9	-7.7	-7.5	-7.2	-6.9	-6.8	-6.7	-5.9	-5.6
Curlone	-7.2	-7.1	-6.8	-6.7	-6.7	-6.6	-6.6	-6.0	-4.9
Cyclocurcumin	39.9	-	-	-	-	-	-	-	-
Demethoxycurcumin	-8.0	-6.7	-6.2	-5.3	-	-	-	-	-
Furanodienone	-8.0	-7.0	-6.8	-6.8	-6.6	-6.6	-6.4	-6.4	-5.7
Germacrone	-7.8	-6.8	-6.4	-6.2	-6.1	-5.7	-5.6	-5.5	-
Hexahydrocurcumin	-7.1	-7.0	-7.0	-6.5	-6.4	-6.2	-5.8	-5.1	-4.8
Hexahydrocurcuminol	-6.5	-5.6	-5.3	-5.1	-5.0	-4.8	-4.7	-	-
Isocurcumenol	-7.8	-7.7	-7.4	-7.2	-6.8	-6.4	-6.1	-5.6	-5.2
Isorhamnetin	-4.9	-4.8	-3.7	-2.2	-	-	-	-	-
P-hydroxybenzoic acid	-5.8	-5.7	-5.6	-5.6	-5.6	-5.5	-5.5	-5.3	-5.3
Quercetin	-7.3	-6.9	-6.8	-4.9	-	-	-	-	-
Sinapic acid	-6.7	-6.6	-6.5	-6.5	-6.5	-6.5	-5.7	-5.4	-5.2
T-cinnamic acid	-5.9	-5.8	-5.7	-5.6	-5.5	-5.4	-5.4	-5.3	-5.2
Turmerone	-6.3	-6.3	-6.2	-6.1	-5.9	-5.7	-5.6	-5.1	-4.9
Vanillic acid	-6.3	-6.3	-5.7	-5.7	-5.6	-5.5	-5.5	-5.5	-5.5
Zederone	-7.9	-7.9	-7.8	-6.7	-6.7	-6.6	-6.1	-6.0	-6.0
Zingiberene	-6.1	-6.0	-5.7	-5.7	-5.6	-5.5	-5.4	-5.4	-5.4

Binding Affinity Value Between Ligands with TPP C-Terminal Domain from *C. albicans*

Molecular docking was run for all 30 ligands, and the TPP output in .pdbqt format. Based on Table 3, the docking of 30 ligands with TPP from *Candida albicans* shows that the anthraquinones resulted in the highest binding affinity of -8.1 kcal/mol. The docking between TPP and three drug controls shows that fluconazole produced the highest binding affinity at -7.9 kcal/mol. Redocking performed by Trehalose resulted in affinity binding of -8.3 kcal/mol. These results indicate that Trehalose possesses the highest binding affinity for TPP from *C. albicans.*

Binding Conformation Based on Hydrogen, Hydrophobic and Electrostatic Interaction Between Ligands and TPP From *C. albicans*

During the analyses, hydrogen-bonded TPP amino acid residues and hydrophobic and electrostatic interactions with ligands were recorded using AutoDock Vina. Figure 7 shows the binding conformation of the compounds using PyMol and Discovery Studio Biovia 2021, while Figures 8, 9, and 10 show the 2D representation of the TPP complex interaction using Discovery Studio Biovia 2021.

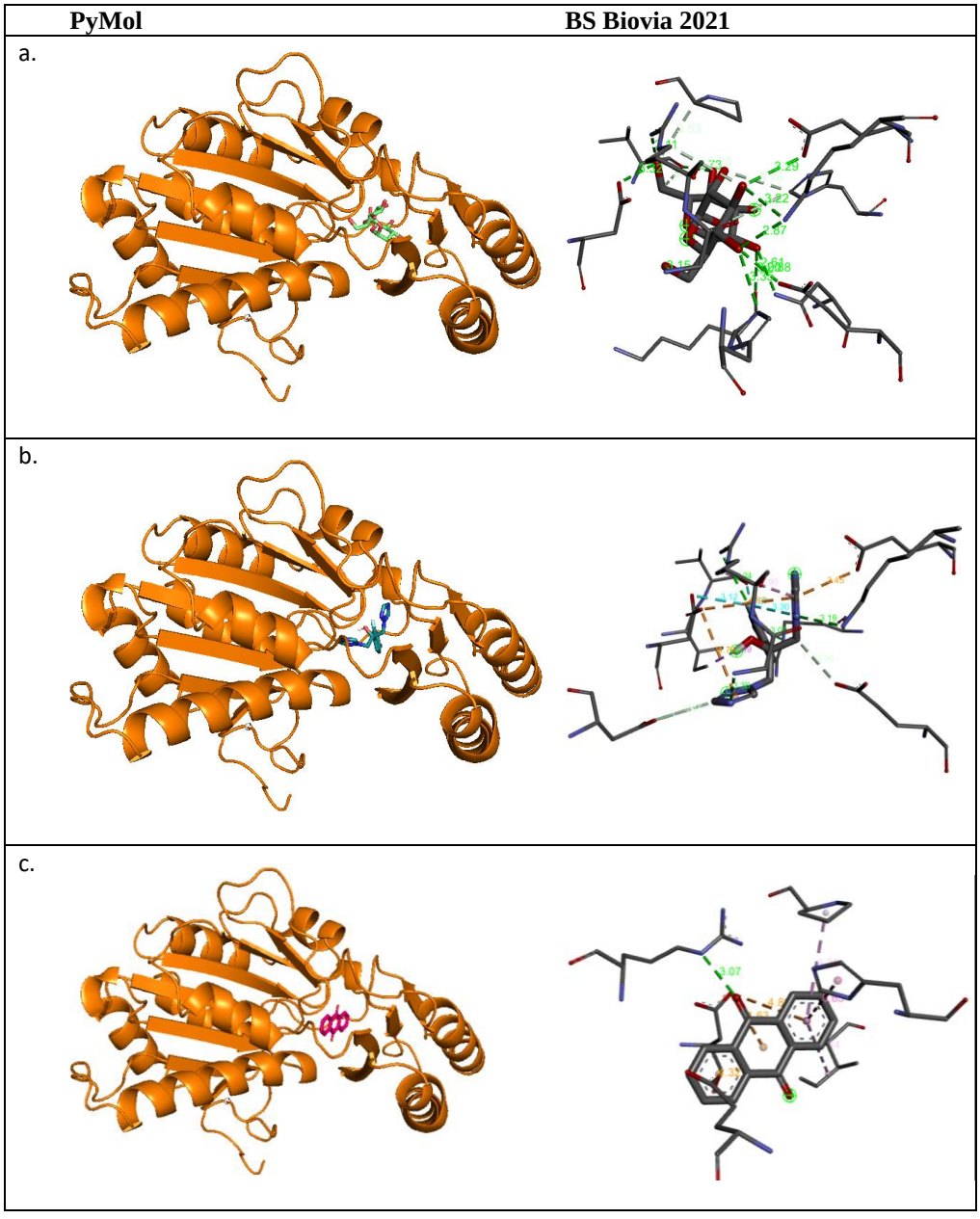

Figure 7. The binding visualization of 5DXI receptors and ligands. a. Trehalose b. Fluconazole c. Anthraquinones.

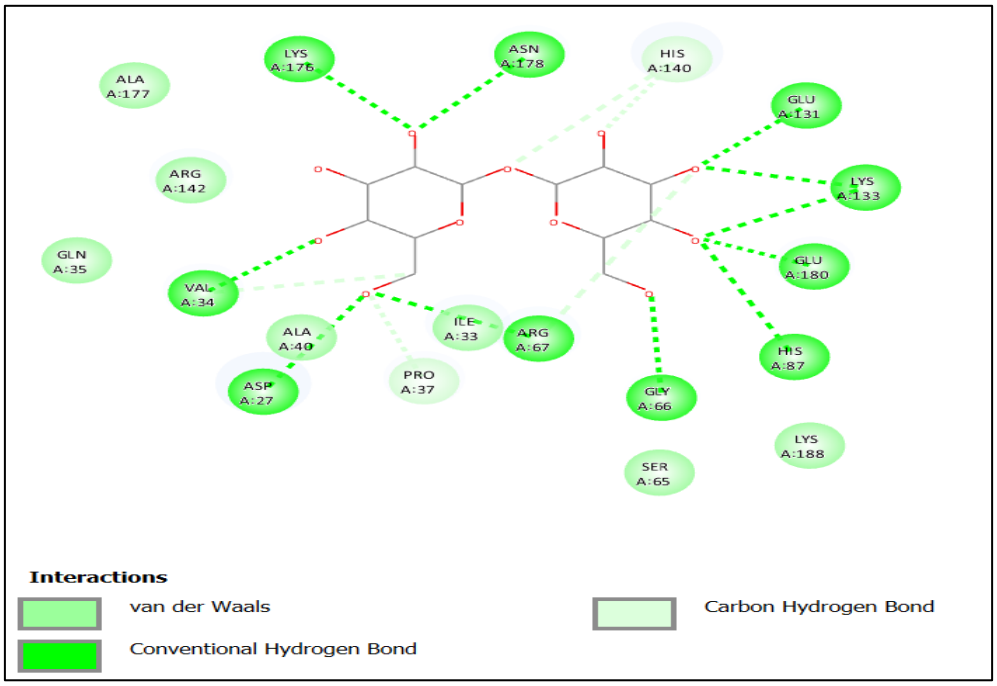

Figure 8. The 2D illustration of docked trehalose-5DXI complex interaction visualization by DS Biovia 2021.

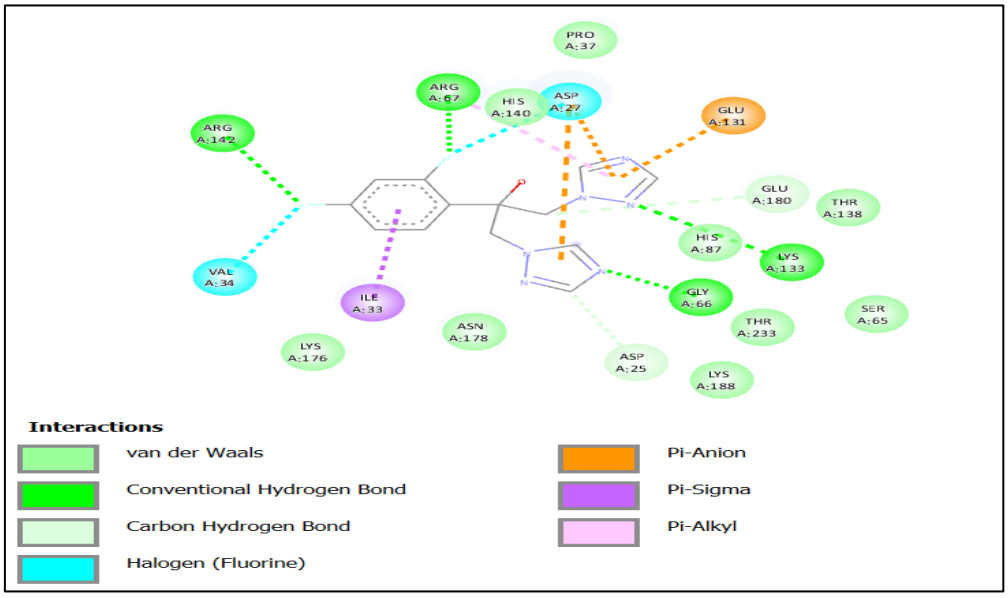

Figure 9. The 2D illustration of docked fluconazole-5DXI complex interaction visualization by Discovery Studio Biovia 2021.

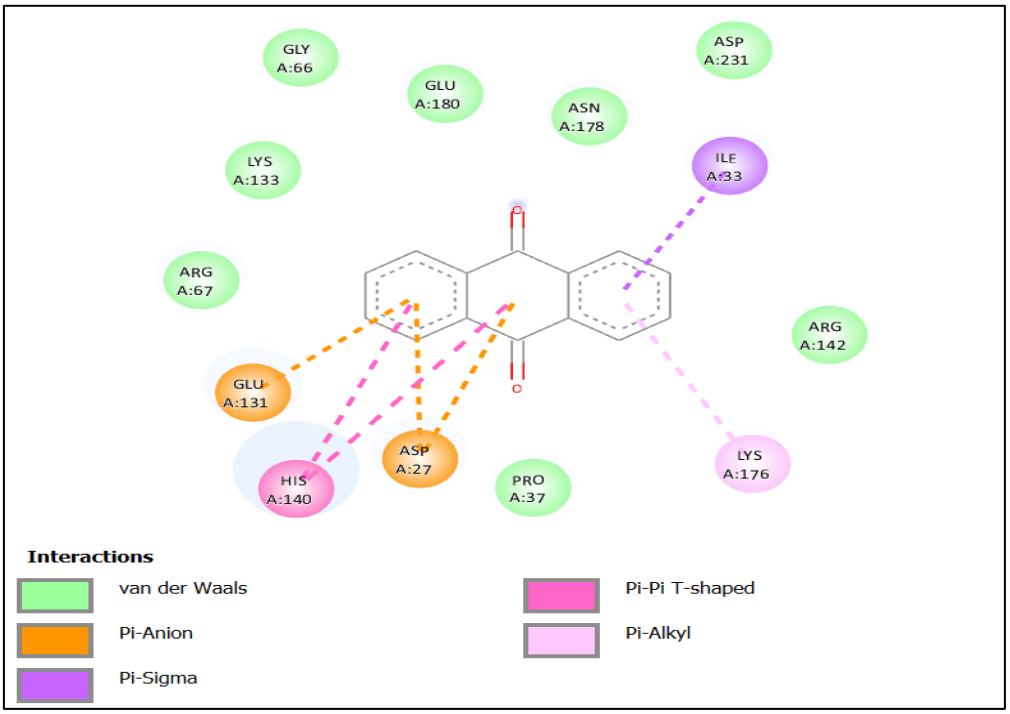

Figure 10. The 2D illustration of docked anthraquinones-5DXI complex interaction visualization by Discovery Studio Biovia 2021.

Table 4. Amino acid residues interact with the ligands and the TPP from C. albicans on hydrogen bonding, hydrophobic, and electrostatic interactions, respectively.

Ligand	Binding affinity, ΔG (kcal/mol)	Amino acids involved and distance (Å)		
		Hydrogen Bonding Interaction	Hydrophobic Interaction	Electrostatic Interaction
Trehalose	-8.3	LYS176 (3.00), VAL34 (2.73), GLU131 (3.29), HIS87 (3.35), GLU180 (2.61), ASP27 (3.32), GLY66 (3.15), ARG67 (3.11), LYS133 (3.22), LYS133 (2.87), ASN178 (2.88), VAL34 (3.62), PRO37 (3.52), ARG67 (3.70), HIS140 (3.77), HIS140 (3.76)	-	-
Fluconazole	-7.9	GLY66 (3.38), ARG67 (3.24), LYS133 (3.19), ARG142 (3.00), GLU180 (3.56), ASP25 (3.46), ASP25 (3.77)	ILE33 (3.99), ASP27 (4.90)	ASP27 (4.87), ASP27 (4.76), GLU131 (3.45)
Anthraquinones	-8.1	ARG67 (3.07)	HIS140 (5.65), ILE33 (5.14), PRO37 (5.20)	ASP27 (4.63), ASP27 (4.86), GLU180 (4.32)

Based on Table 4, trehalose redocking interaction with 5DXI receptor were supported by 16 hydrogen bonds at residues LYS176 (3.00 Å), VAL34 (2.73 Å), GLU131 (3.29 Å), HIS87 (3.35 Å), GLU180 (2.61 Å), ASP27 (3.32 Å), GLY66 (3.15 Å), ARG67 (3.11 Å), LYS133 (3.22 Å), LYS133 (2.87 Å), ASN178 (2.88 Å), VAL34 (3.62 Å), PRO37 (3.52 Å), ARG67 (3.70 Å), HIS140 (3.77 Å) and HIS140 (3.76 Å). There were no hydrophobic interactions, and electrostatic interactions were identified.

Fluconazole compounds formed seven hydrogen bonds with the 5DXI receptor, involving amino acids GLY66 (3.38 Å), ARG67 (3.24 Å), LYS133 (3.19 Å),

ARG142 (3.00 Å), GLU180 (3.56 Å), ASP25 (3.46 Å) and ASP25 (3.77 Å). Meanwhile, two hydrophobic interactions occurred involving amino acids ILE33 and ASP27 with a distance of 3.99 Å and 4.90 Å, respectively. The interaction between fluconazole and TPP results in three electrostatic interactions involving amino acids of ASP27 (4.87 Å), ASP27 (4.76 Å), and GLU131 (3.45 Å).

Next, the interaction between anthraquinones and the 5DXI receptor formed a hydrogen bond involving the amino acid ARG67 with 3.07 Å. Hydrophobic interactions also occur involving the amino acids HIS140 (5.65 Å), ILE33 (5.14 Å), and PRO37 (5.20 Å). There were three amino acids for electrostatic interaction between anthraquinones compound and TPP, which are ASP27 (4.63 Å), ASP27 (4.86 Å) and GLU180 (4.32 Å).

Molecular Docking Results Between *Curcuma longa* Phytochemicals and TPP Receptor from *Salmonella typhimurium* in Complex with Trehalose (PDB: 6UPD)

The next docking validation was performed by redocking all *Curcuma longa* ligands with the receptor of trehalose-6-phosphate phosphatase in complex with trehalose from *Salmonella typhimurium* (PDB: 5DX9). Redocking was executed with a grid box of size x=6, y=10, z=8, and center x=-0.945, y=19.060, z=55.080 at 1,000 Angstroms (Å).

Figure 11 below shows the results of the redocking inhibitor Trehalose (blue) and the crystal conformation of Trehalose (green). The superimposition fits between the redocking ligand (blue) and the crystal conformation (green), which describes the position of the binding site between the ligand and the receptor. The RMSD value is 0.570 Å. RMSD has often been used to measure the quality of reproduction of a known crystallographic binding pose by a computational method. The lower the RMSD represents a good reproduction of the correct binding pose.

Binding Affinity Value Between Ligands with TPP from *S. typhimurium* in Complex with Trehalose

Molecular docking was run for all 30 ligands and the TPP output, both in .PDBQT format. Based on Table 5, the docking of 30 ligands with TPP from *Salmonella typhimurium* shows that the anthraquinones resulted in the highest binding affinity of -7.5 kcal/mol. The docking between TPP and three drugs control, fluconazole produced the highest binding affinity, which is -7.4 kcal/mol, and redocking performed by trehalose resulted in affinity binding of -8.7 kcal/mol. These results indicate that trehalose possesses the highest binding affinity for TPP from *S. typhimurium.*

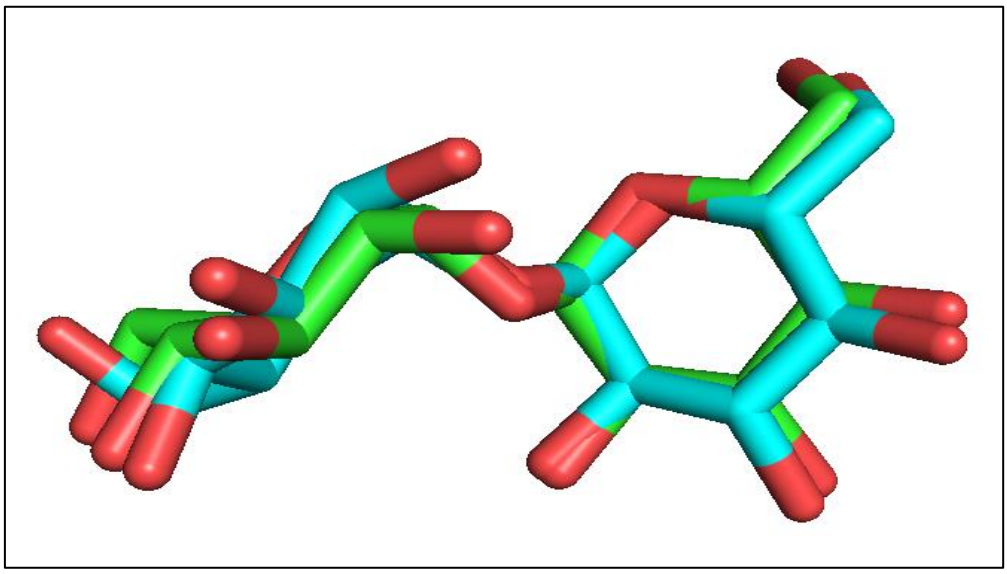

Figure 11. Redocked (yellow) and the crystal structure of trehalose (pink).

Table 5. The binding affinity of ligand molecules to modelled TPP, 6UPD using *AutoDock Vina*.

Ligand	Binding energy (binding affinity) generated between ligand and TPP receptor in each form, ΔG (kcal/mol)								
	1	**2**	**3**	**4**	**5**	**6**	**7**	**8**	**9**
Trehalose	-8.7	-8.6	-7.0	-6.8	-6.8	-6.7	5.7	-	-
Fluconazole	-7.4	-7.3	-7.3	-7.1	-6.8	-6.8	-6.3	-5.8	-4.4
Ampicillin	-7.0	-5.0	-4.8	-4.7	-4.3	-	-	-	-
Isoniazid	-5.3	-5.2	-5.0	-4.9	-4.9	-4.8	-4.8	-4.8	-4.8
Anthraquinones	-7.5	-7.5	-7.4	-7.4	-6.5	-6.5	-6.5	-6.3	-5.9
Ar-tumerone	-6.5	-6.3	-6.3	-6.3	-5.9	-5.9	-5.7	-5.7	-5.7
Bisacurone	-7.4	-6.7	-6.5	-6.4	-6.4	-6.1	-6.1	-5.8	-5.5
Bisdemethoxycurcumin	-6.7	-6.7	-6.4	-6.2	-4.5	-	-	-	-
Borneol	-5.5	-5.4	-5.3	-5.3	-5.2	-5.2	-5.2	-5.1	-5.1
Caffeic acid	-6.3	-6.2	-6.1	-6.0	-5.9	-5.9	-5.8	-5.7	-5.6
Cis-curcumin	-6.9	-5.9	-4.5	-4.4	-	-	-	-	-
Coumaric	0.8	-	-	-	-	-	-	-	-
Coumarin	-5.8	-5.7	-5.6	-5.5	-5.5	-5.5	-5.5	-5.4	-5.4
Curcumin	-5.5	-3.6	-	-	-	-	-	-	-
Curcumin Beta-D-glucuronide	20.6	-	-	-	-	-	-	-	-
Curcuphenol	-6.2	-5.9	-5.9	-5.8	-5.7	-5.7	-5.6	-5.6	-5.5
Curdione	-7.1	-6.6	-5.5	-5.4	-5.2	-4.8	-4.8	-4.3	-
Curlone	-6.1	-6.0	-5.9	-5.8	-5.8	-5.7	-5.7	-5.4	-5.4
Cyclocurcumin	33	-	-	-	-	-	-	-	-
Demethoxycurcumin	-7.2	-6.5	-5.0	-4.4	-	-	-	-	-
Furanodienone	-7.1	-6.4	-6.2	-6.2	-6.1	-5.9	-5.4	-4.9	-4.6
Germacrone	-6.2	-6.2	-6.0	-5.2	-4.6	-4.6	-4.2	-3.8	-
Hexahydrocurcumin	-5.9	-5.7	-4.9	-4.2	-4.2	-	-	-	-
Hexahydrocurcuminol	-5.6	-5.4	-4.9	-4.7	-4.6	-4.3	-3.9	-3.7	-
Isocurcumenol	-6.8	-6.2	-6.2	-6.0	-6.0	-6.0	-5.9	-5.8	-5.5
Isorhamnetin	-6.2	-5.6	-5.1	-5.1	-3.7	-3.2	-	-	-
P-hydroxybenzoic acid	-5.5	-5.4	-5.3	-5.3	-5.3	-5.2	-5.0	-5.0	-5.0
Quercetin	-6.2	-5.8	-4.1	-3.6	-	-	-	-	-
Sinapic acid	-6.5	-6.3	-6.3	-6.1	-6.1	-5.9	-5.9	-5.9	-5.5
T-cinnamic acid	-5.5	-5.5	-5.3	-5.3	-5.3	-5.0	-4.9	-4.9	-4.8
Turmerone	-6.5	-6.3	-6.1	-6.1	-6.1	-6.0	-5.8	-5.6	-5.5
Vanillic acid	-5.9	-5.9	-5.7	-5.7	-5.7	-5.5	-5.5	-5.3	-5.2
Zederone	-6.0	-6.0	-5.9	-5.5	-5.2	-3.7	3.2	-	-
Zingiberene	-5.4	-5.3	-5.3	-5.3	-5.2	-5.1	-5.1	-5.0	-4.9

Hydrogen, Hydrophobic and Electrostatic Interactions between Ligands and TPP from *S. typhimurium* in Complex with Trehalose

During the analyses, hydrogen-bonded TPP amino acid residues and hydrophobic and electrostatic interactions with ligands were recorded using AutoDock Vina. Figure 12 shows the binding conformation of the compounds using PyMol and Discovery Studio Biovia 2021, while Figure 13, Figure 14, and Figure 15 shows the 2D representation of the TPP complex interaction using Discovery Studio Biovia 2021.

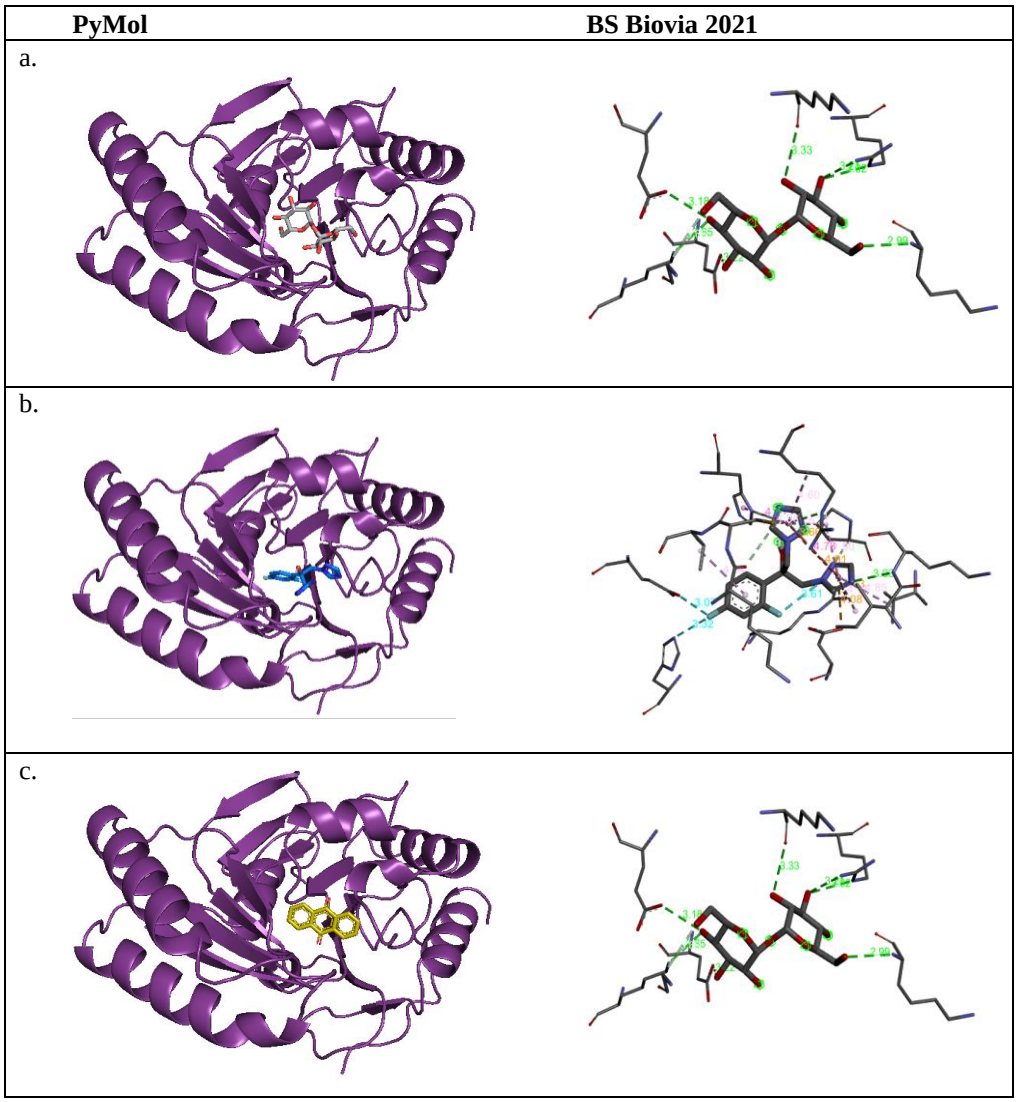

Figure 12. The binding visualization of 6UPD receptor and ligands.
a. Trehalose b. Fluconazole c. Anthraquinones.

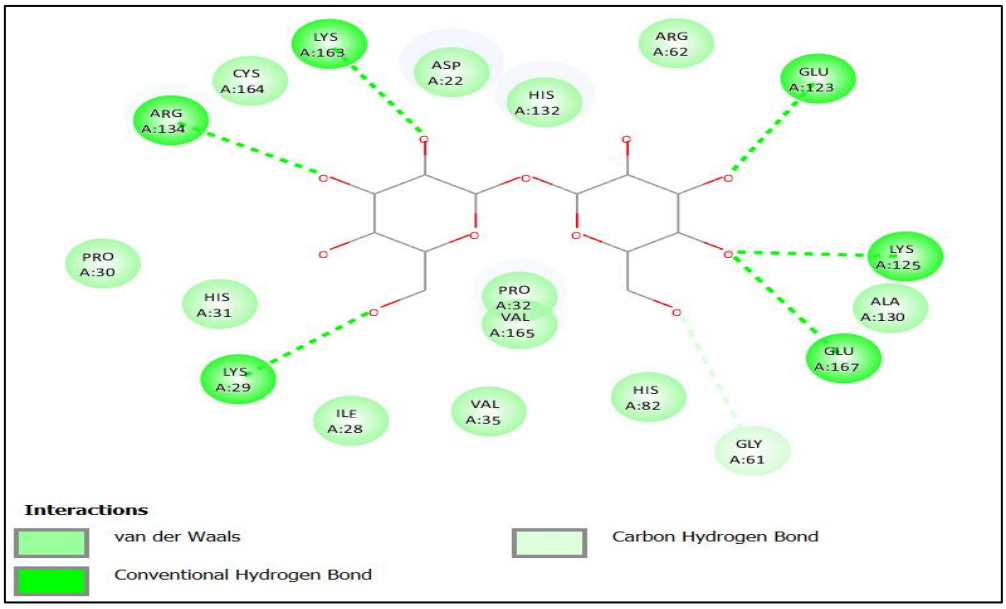

Figure 13. The 2D illustration of docked trehalose-6UPD complex interaction visualization using Discovery Studio Biovia 2021.

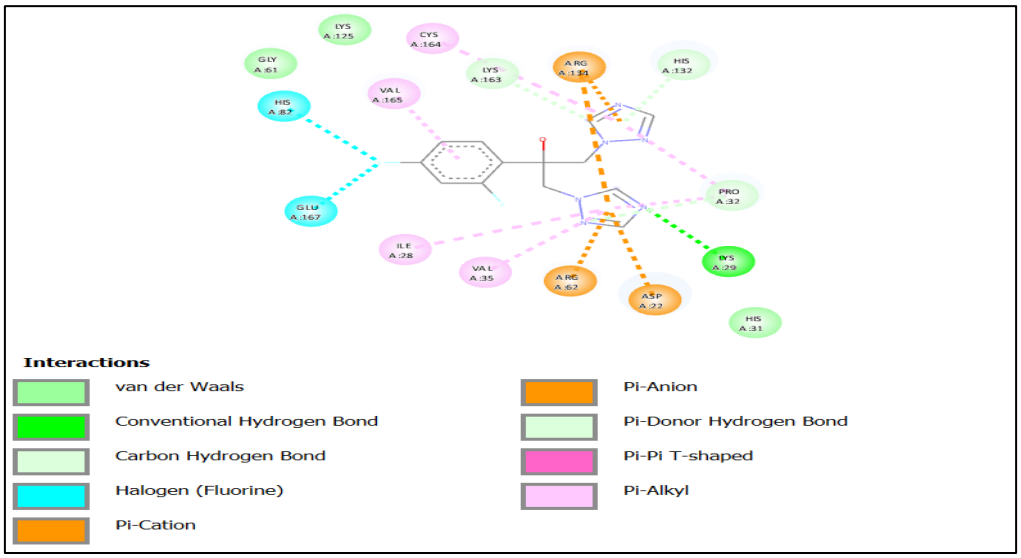

Figure 14. The 2D illustration of docked fluconazole-6UPD complex interaction visualization using Discovery Studio Biovia 2021.

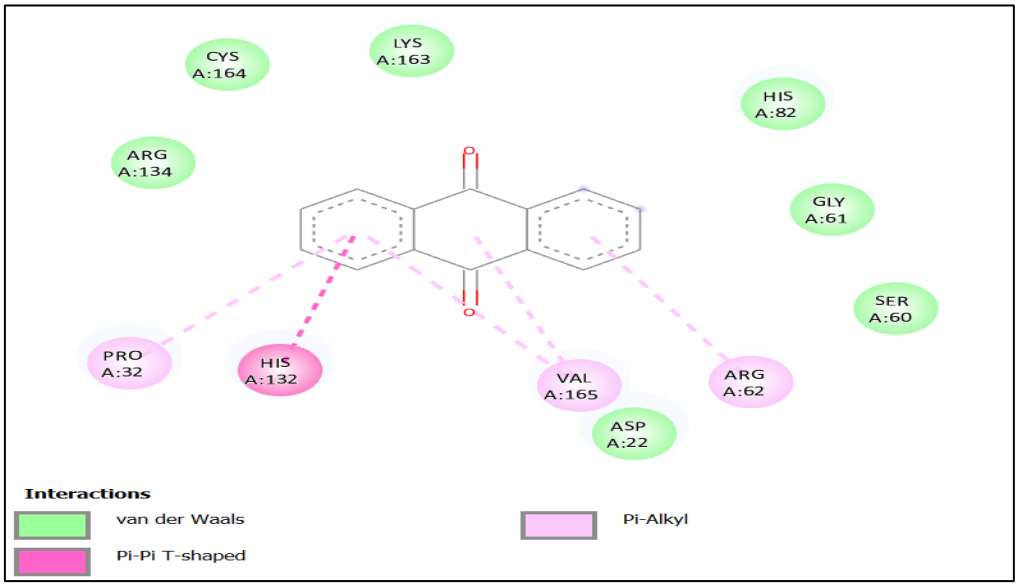

Figure 15. The 2D illustration of docked anthraquinones-6UPD complex interaction visualization using Discovery Studio Biovia 2021.

Based on Table 6, trehalose redocking interaction with 6UPD receptor were supported by eight hydrogen bonds at residues LYS125 (3.33 Å), GLU123 (3.22 Å), GLU167 (3.18 Å), LYS29 (2.99 Å), LYS125 (2.85 Å), ARG134 (3.02 Å), ARG134 (3.21 Å) and GLY61 (3.66 Å). There were no hydrophobic or electrostatic interactions found between the trehalose molecule and 6UPD.

Fluconazole compounds formed six hydrogen bonds with the 6UPD receptor, involving amino acids LYS29 (3.03 Å), UNK0 (3.79 Å), PRO32 (3.25 Å), ARG134 (3.66 Å), HIS132 (3.42 Å) and ARG134 (3.39 Å). Hydrophobic interactions also occurred involving amino acids LYS163 (4.78 Å), HIS132 (4.54 Å), VAL165 (4.34 Å), ILE28 (4.95 Å), PRO32 (4.90 Å), VAL35 (4.85 Å), PRO32 (5.27 Å), ARG134 (4.60 Å) and CYS164 (4.98 Å). Three electrostatic interactions were also identified with ARG62 (4.43 Å), ARG134 (4.91 Å), and ASP22 (4.08 Å).

Lastly, the interaction between anthraquinones and the 6UPD receptor did not result in hydrogen interaction. Six hydrophobic interactions occur involving the amino acids HIS132 (4.66 Å), ILE28 (5.18 Å), PRO32 (5.12 Å), PRO32 (5.23 Å), ALA130 (5.22 Å) and VAL165 (4.66 Å). Meanwhile, two electrostatic interactions occurred involving amino acids ASP22 (4.12 Å) and ASP22 (4.03 Å).

Table 6. Amino acid residues interact with the ligands and the TPP from S. typhimurium on hydrogen bonding, hydrophobic interactions, and electrostatic interactions, respectively.

Ligand	Binding affinity, ΔG (kcal/mol)	Amino acids involved and distance (Å)		
		Hydrogen Bonding Interaction	Hydrophobic Interaction	Electrostatic Interaction
Trehalose	-8.7	LYS125 (3.33), GLU123 (3.22), GLU167 (3.18), LYS29 (2.99), LYS125 (2.85), ARG134 (3.02), ARG134 (3.21), GLY61 (3.66)	-	-
Fluconazole	-7.4	LYS29 (3.03), LYS163 (3.79), PRO32 (3.25), ARG134 (3.66), HIS132 (3.42), ARG134 (3.39)	LYS163 (4.78), HIS132 (4.54), VAL165 (4.34), ILE28 (4.95), PRO32 (4.90), VAL35 (4.85), PRO32 (5.27), ARG134 (4.60), CYS164 (4.98)	ARG62 (4.43), ARG134 (4.91), ASP22 (4.08)
Anthraquinones	-7.5	-	HIS132 (4.66), ILE28 (5.18), PRO32 (5.12), PRO32 (5.23), ALA130 (5.22), VAL165 (4.66)	ASP22 (4.12), ASP22 (4.03)

Quercetin and Anthraquinones are the Potential Phytochemicals That Can Suppress TPP Protein

According to the view of a previous study [22], the phytochemicals anthraquinone and quercetin can be potential competitive inhibitors because these phytochemicals bind to the active site of the TPP enzyme, where all these phytochemicals bind to one or more motifs through steric hindrance. Steric hindrance prevents further interaction of the natural substrate with the receptor when a competitive inhibitor binds to the active site. This effect of steric hindrance means that when phytochemicals bind to the active site of the TPP enzyme, the TPP enzyme cannot catalyze T6P to trehalose [22].

As stated in a study done previously [22], 3D quercetin is surrounded by amino acids of the target protein, SARS-CoV-2 main protease 3CL. Amino acids ASN72, ALA70, LYS97, and GLY15 formed the conventional hydrogen bond, hydrocarbon, Pi cation, and Pi alkyl interactions between quercetin and SARS-CoV-2 major protease 3CL. In addition, several recent pharmacological online studies have predicted that quercetin is the most potential compound for treating COVID-19 as an herbal formulation or decoction [22]. These findings suggested that quercetin may also be a potential anti-microbial against trehalose-6-phosphate phosphatase of pathogenic microbes.

Next, the inhibitory effect of four anthraquinones, including chrysophanol, emodin, fission, and rhein, on tyrosinase was investigated by enzyme inhibition assay [23]. Four histidine residues, including His61, His 85, His259, and His263, were involved in the binding of tyrosinase to chrysophanol. Thus, three residues (His85, His259, and His263), four residues (His61, His85, His259, and His296), and six residues (HIS61, HIS85, HIS94, HIS259, HIS263, AND HIS296) were found to be associated with tyrosinase binding emodin, physcion and rhein, respectively [23].

In addition to histidine residues, anthraquinones were found to surround other amino acid residues, including hydrophobic and hydrophilic amino acids, indicating that the interactions between anthraquinones and tyrosinase were electrostatic forces and hydrophobic interactions in nature [23]. Due to the presence of aromatic rings in the structure of anthraquinone compounds, several σ-π and π-π conjugated structures were formed between these rings and amino acid residues. The results showed that anthraquinones competitively inhibited tyrosinase activity and spontaneously bound to tyrosinase in one binding site by a static process involving electrostatic force, hydrophobic interaction, and hydrogen bonding [23].

Molecular Docking Studies

Molecular docking is becoming a popular approach in researching and developing new drugs. It is an effective tool for structure-activity relationship analysis [10,24]. This approach allows the prediction of the binding conformation and binding energy of a small molecule ligand to a target protein, which then facilitates the identification of a potential ligand for pharmaceutical use. In addition, molecular docking saves time and costs compared to traditional laboratory experiments [10].

The binding energy (ΔG) is obtained during the docking process, a parameter of the conformational stability between the ligand and the receptor. Interacting ligands and receptors are usually in the lowest energy state, where protein-ligand binding occurs spontaneously [10]. This state causes the molecule to be in a stable state. Therefore, the lower the ΔG value, the more stable the ligand-receptor interaction. It follows that both protein folding and protein-ligand binding occur when ΔG is low in the system. Thus, negative ΔG scores indicate the stability of emerging complexes with receptor molecules, an important property of effective drugs [11].

Non-Covalent Molecular Interactions

Hydrogen bonding, hydrophobic, and electrostatic interactions contribute to different binding affinity values during ligand-protein docking with TPP protein. Hydrophobic interactions are crucial for protein stability, while electrostatic interactions affect structure, chemical properties, stability, and biological reactivity. Hydrogen bonding helps maintain protein folding configurational equilibrium, while electrostatic interactions affect binding affinity, structure, and chemical properties.

TPP receptor (PDB:5DX9) exhibits strong interaction with the following ligands with high binding affinity: T6P inhibitor (-10.4 kcal/mol), fluconazole (-8.8 kcal/mol), and quercetin (-9.3 kcal/mol) based on Table 1. The best binding affinity is obtained with the T6P inhibitor. T6P results in a binding affinity of 14 hydrogen interactions significantly greater than that produced by quercetin, five hydrogen interactions, and ampicillin, eight hydrogen interactions. Quercetin and fluconazole ligands interact with the same residue in the TPP receptor pursuant to a hydrogen bond (Lys176) and a hydrophobic interaction (Pro36), which does not apply to T6P inhibitor interaction. Even though T6P has a strong affinity, quercetin had the same binding affinity of -9.3 kcal/mol, the second highest of these three ligands. Therefore, quercetin could potentially be an effector of TPP activity.

Next, in this study, the ligand-protein interaction of TPP from *C. albicans* (PDB: 5DXI) with a binding affinity of -8.3 kcal/mol, trehalose docking has eight hydrogen bonds, and no hydrophobic and electrostatic interaction was recorded. Hence, anthraquinones had a higher binding affinity than fluconazole, which acts as the drug control of -8.1 and -7.9 kcal/mol, respectively. In addition, fluconazole has higher hydrogen and electrostatic interactions than anthraquinones (Table 3). In contrast, anthraquinones with three amino acids involved in hydrophobic interaction had higher hydrophobic interaction than fluconazole, which contributes only two amino acids. This means that all types of interactions jointly contributed to the binding affinity values.

The interaction between trehalose, fluconazole, and anthraquinones for the TPP receptor from *S. typhimurium* (PDB: 6UPD) resulted in binding affinities of -8.7, -7.4, and -7.5 kcal/mol, respectively as shown on Table 5. Trehalose gives the best binding affinity due to the highest hydrogen bond in the ligand-receptor interaction. The ligand interaction of anthraquinones and fluconazole interact with the same amino acid residue for a hydrophobic interaction (Ile28, Pro32, and Val65). Even though trehalose inhibitor had the highest affinity binding, anthraquinones still have a good affinity higher than the drug control, fluconazole, so it is expected to be used as a TPP effector.

Drug Effectiveness

In docking studies, free energy (δG) determines protein-ligand complex binding affinity using AutoDock Vina 4.2 drug finder. A negative value indicates strong affinity, while a favorable conformation indicates favorable binding. The docking accuracy is set to standard accuracy and flexible ligand docking mode. All interaction studies showed binding of the leads to the conserved active site region 3, indicating the importance of this region because it is specific for Mg binding and the active site of a significant part of TPPs [1]. Thus, work on TPP inhibition presents a chance to develop new-generation drugs like ampicillin, fluconazole, and isoniazid to treat or control pathogen toxicity. Phytochemicals from plant sources are promising agents for drug development, with *in silico* studies facilitating the screening of potent inhibitors. These phytochemical components can act as new-generation drugs or inhibitors for diseases like tuberculosis, fungal infections, elephantiasis, and meningitis [1].

The Design of Drug Molecules

As mentioned by [25], docking and structure-based drug molecule design relies on accurate information about the active site architecture, which determines the three-dimensional geometry and direct and indirect interactions. Target proteins may have multiple pockets or cavities for ligand binding, but their exact architecture is unclear from structural data. Variations in the shape and size of the binding pocket can occur due to amino acid side chains, backbone motions, loop motions, and ligand-induced conformational changes. The docking process remains uncertain due to the dynamic physicochemical properties of protein-ligand systems.

Developing various docking techniques that consider the flexibility of protein-ligand interactions and their various binding conformations has also been facilitated by computational, proteomics, and genomics developments. Receptor flexibility explains more precise predictions of binding poses and a more logical representation of protein-ligand binding interactions. Protein flexibility has been considered when creating protein ensembles or using dynamic

docking techniques. Dynamic docking completely analyses drug-receptor binding and recognition from both an energetic and mechanistic point of view, as well as solvation and entropic consequences. Dynamic docking is computationally expensive, yet it is increasingly utilized in quick drug development programs to screen vast compound libraries for promising medicines [25].

CONCLUSION

To conclude, phytochemicals from *Curcuma longa* can potentially act as potential inhibitors of target TPP proteins supported by high binding affinities and various binding interactions such as hydrogen bonding interactions, hydrophobic interactions, and electrostatic interactions, which induce trehalose signaling pathways. However, to validate these *in silico* results, additional in vitro and in vivo research is required.

In the author's findings, the C. longa, quercetin, and ampicillin ligands have the highest binding, corresponding to -8.8 ΔG and -9.3 ΔG for the protein-ligand interaction of TPP from *C. neoformans*. The second protein-ligand interaction from TPP of *C. albicans* between anthraquinones (-8.1 ΔG) and fluconazole (-7.9 ΔG) results in the highest binding affinity compared to the other ligands. This protein-ligand interaction from TPP of *C. albicans* shared almost equivalent results with TPP from *S. typhimurium* interaction, which are -7.5 ΔG and -7.4 ΔG binding affinity for anthraquinones and fluconazole. Despite the differences in binding affinity values, anthraquinones, and fluconazole have their appeal and the highest binding affinity for both TPP from *C. albicans* and *S. typhimurium*.

REFERENCES

1. Umesh, H. R., Ramesh, K. V. & Devaraju, K. S. (2020) Molecular Docking Studies of Phytochemicals Against Trehalose-6-Phosphate Phosphatases of Pathogenic Microbes. *Beni-Suef University Journal of Basic and Applied Sciences*, **9(1)**.

2. Li, J., Fu, A. & Zhang, L. (2019) An Overview of Scoring Functions Used for Protein– Ligand Interactions in Molecular Docking. *Interdisciplinary Sciences: Computational Life Sciences*, **11(2)**, 320–328.

3. Chen, X., Abubakar, Y. S., Yang, C., Wang, X., Miao, P., Lin, M., Wen, Y., Wu, Q., Zhong, H., Fan, Y., Zhang, M., Wang, Z., Zhou, J. & Zheng, W. (2021) Trehalose Phosphate Synthase Complex-Mediated Regulation of Trehalose-6-Phosphate Homeostasis Is Critical for Development and Pathogenesis in *Magnaporthe oryzae*. *MSystems*, **6(5)**.

4. Yuan, S., Wei, X., Wang, S., & Wang, J. (2020). Characterization of Trehalose-6-Phosphate Phosphatase in Trehalose Biosynthesis, Asexual Development, Stress Resistance and Virulence of An Insect Mycopathogen. *Pesticide Biochemistry and Physiology*, **163**, 185–192.

5. Micoli, F., Bagnoli, F., Rappuoli, R. & Serruto, D. (2021) The Role of Vaccines in Combatting Antimicrobial Resistance. *Nature Reviews Microbiology*, **19(5)**, 287–302.

6. Adamczak, A., Ożarowski, M. and Karpiński, T. M. (2020) Curcumin, A Natural Antimicrobial Agent with Strain-Specific Activity. *Pharmaceuticals*, **13(7)**, 153.

7. Hussain, Y., Alam, W., Ullah, H., Dacrema, M., Daglia, M., Khan, H. & Arciola, C. R. (2022) Antimicrobial Potential of Curcumin: Therapeutic Potential and Challenges to Clinical Applications. *Antibiotics (Basel, Switzerland)*, **11(3)**, 322.

8. Oyinloye, B. E., Adekiya, T. A., Aruleba, R. T., Ojo, O. A. & Ajiboye, B. O. (2019) Structure-Based Docking Studies of GLUT4 Towards Exploring Selected Phytochemicals from *Solanum xanthocarpum* As a Therapeutic Target for The Treatment of Cancer. *Current Drug Discovery Technologies*, **16(4)**, 406–416.

9. Tutumlu, G., Dogan, B., Avsar, T., Orhan, M. D., Calis, S. & Durdagi, S. (2020) Integrating Ligand and Target-Driven Based Virtual Screening Approaches With In Vitro Human Cell Line Models and Time-Resolved Fluorescence Resonance Energy Transfer Assay to Identify Novel Hit Compounds Against TPP. *Frontiers in Chemistry*, **8**, 167.

10. Abdullah, M. Z., Bakar, L. M., Arief Ichwan, S. J., Othman, N. & Taher, M. (2022) Molecular Docking Study of Naturally Derived β-mangostin with Antiapoptotic TPP Proteins Toward Oral Cancer Treatment. ESTEEM *Academic Journal*, **18**, 128–138.

11. Afriza, D., Suriyah, W. H. & Ichwan, S. J. A. (2018) *In Silico* Analysis of Molecular Interactions Between the Anti-Apoptotic Protein Survivin and Dentatin, Nordentatin, and Quercetin. *Journal of Physics: Conference Series*, **1073(3)**, 032001.

12. Vanaporn, M. and Titball, R. W. (2020) Trehalose and Bacterial Virulence. *Virulence*, **11(1)**, 1192–1202.

13. Assoni, G., Frapporti, G., Colombo, E., Gornati, D., Posadas, I., Polito, L., Seneci, P., Piccoli, G. & Arosio, D. (2021) Trehalose-Based Neuroprotective Autophagy Inducers. *Bioorganic & Medicinal Chemistry Letters*, **40**, 127929–127929.

14. Schwarz, S. & Van Dijck, P. (2016) Trehalose Metabolism: A Sweet Spot for *Burkholderia pseudomallei* Virulence. *Virulence*, **8(1)**, 5–7.

15. MacIntyre, A. M., Barth, J. X., Pellitteri, M. C., Scarlett, C. O., Genin, S. & Allen, C. (2020) Trehalose Synthesis Contributes to Osmotic Stress Tolerance and Virulence of the Bacterial Wilt Pathogen *Ralstonia solanacearum*. *Molecular Plant-Microbe Interactions*, **33(3)**, 462–473.

16. Pinzi, L. & Rastelli, G. (2019) Molecular docking: shifting paradigms in drug discovery. *International Journal of Molecular Sciences*, **20(18)**, 4331.

17. Wang, Z., Zhang, P., Ding, X., Wang, J., Sun, Y., Yin, C., Wang, W., Fan, C. & Sun, D. (2021) Co-Delivery of Ampicillin and B-Lactamase Inhibitor by Selenium Nanocomposite to Achieve Synergistic Anti-Infective Efficiency Through Overcoming Multidrug Resistance. *Chemical Engineering Journal*, **414**, 128908.

18. Cavassin, F. B., Baú-Carneiro, J. L., Vilas-Boas, R. R. & Queiroz-Telles, F. (2021) Sixty years of Amphotericin B: An Overview of the Main Antifungal Agent Used to Treat Invasive Fungal Infections. *Infectious Diseases and Therapy*, **10(1)**, 115–147.

19. Bhardwaj, P., Biswas, G. P., Nibedita Mahata, Susanta Ghanta & Biswanath Bhunia (2022) Exploration of Binding Mechanism of Triclosan Towards Cancer Markers Using Molecular Docking and Molecular Dynamics. *Chemosphere*, **293**, 133550–133550.

20. Dasgupta, S. & Bandyopadhyay, M. (2021) Molecular Docking of SARS-COV-2 Spike Epitope Sequences Identifies Heterodimeric Peptide-Protein Complex Formation with Human Zo-1, TLR8 and Brain Specific Glial Proteins. *Medical Hypotheses*, **157**, 110706.

21. Bender, B. J., Gahbauer, S., Luttens, A., Lyu, J., Webb, C. M., Stein, R. M., Fink, E. A., Balius, T. E., Carlsson, J., Irwin, J. J. & Shoichet, B. K. (2021) A Practical Guide to Large-Scale Docking. *Nature Protocols*, **16(10)**, 4799–4832.

22. Gu, Y. -Y., Zhang, M., Cen, H., Wu, Y. -F., Lu, Z., Lu, F., Liu, X. -S. & Lan, H. -Y. (2021) Quercetin as a Potential Treatment for COVID-19-Induced Acute Kidney Injury: Based on Network Pharmacology and Molecular Docking Study. *PLOS ONE*, **16(1)**, e0245209.

23. Zeng, H., Sun, D., Chu, S., Zhang, J., Hu, G. & Yang, R. (2020) Inhibitory Effects of Four Anthraquinones on Tyrosinase Activity: Insight from Spectroscopic Analysis and Molecular Docking. *International Journal of Biological Macromolecules*, **160**, 153–163.

24. Nordin, N., Abd Ghani, M. F. & Othman, R. (2020) Molecular Docking Study of Naturally Derived Flavonoids with Antiapoptotic BCL-2 and BCL-XL Proteins Toward Ovarian Cancer Treatment. *Journal of Pharmacy and Bioallied Sciences*, **12(6)**, 676.

25. Jakhar, R., Dangi, M., Khichi, A. & Chhillar, A. K. (2020) Relevance of Molecular Docking Studies in Drug Designing. *Current Bioinformatics*, **15(4)**, 270–278.